

**Cell Reports, Volume 37**

**Supplemental information**

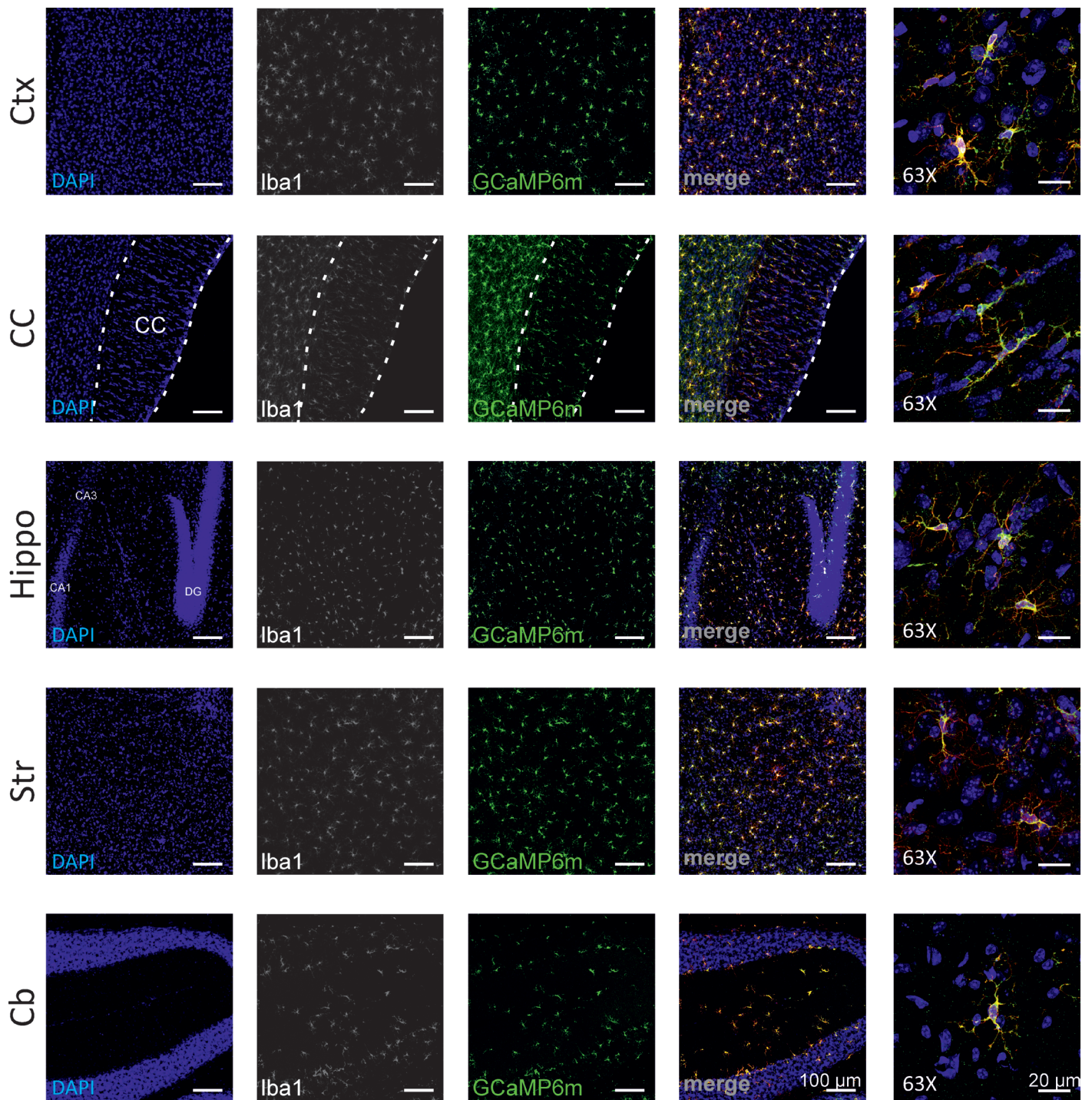
**Microglia sense neuronal activity  
via GABA in the early postnatal hippocampus**

**Francesca Logiacco, Pengfei Xia, Svilen Veselinov Georgiev, Celeste Franconi, Yi-Jen Chang, Bilge Ugursu, Anje Sporbart, Ralf Kühn, Helmut Kettenmann, and Marcus Semtner**

# Supplementary information

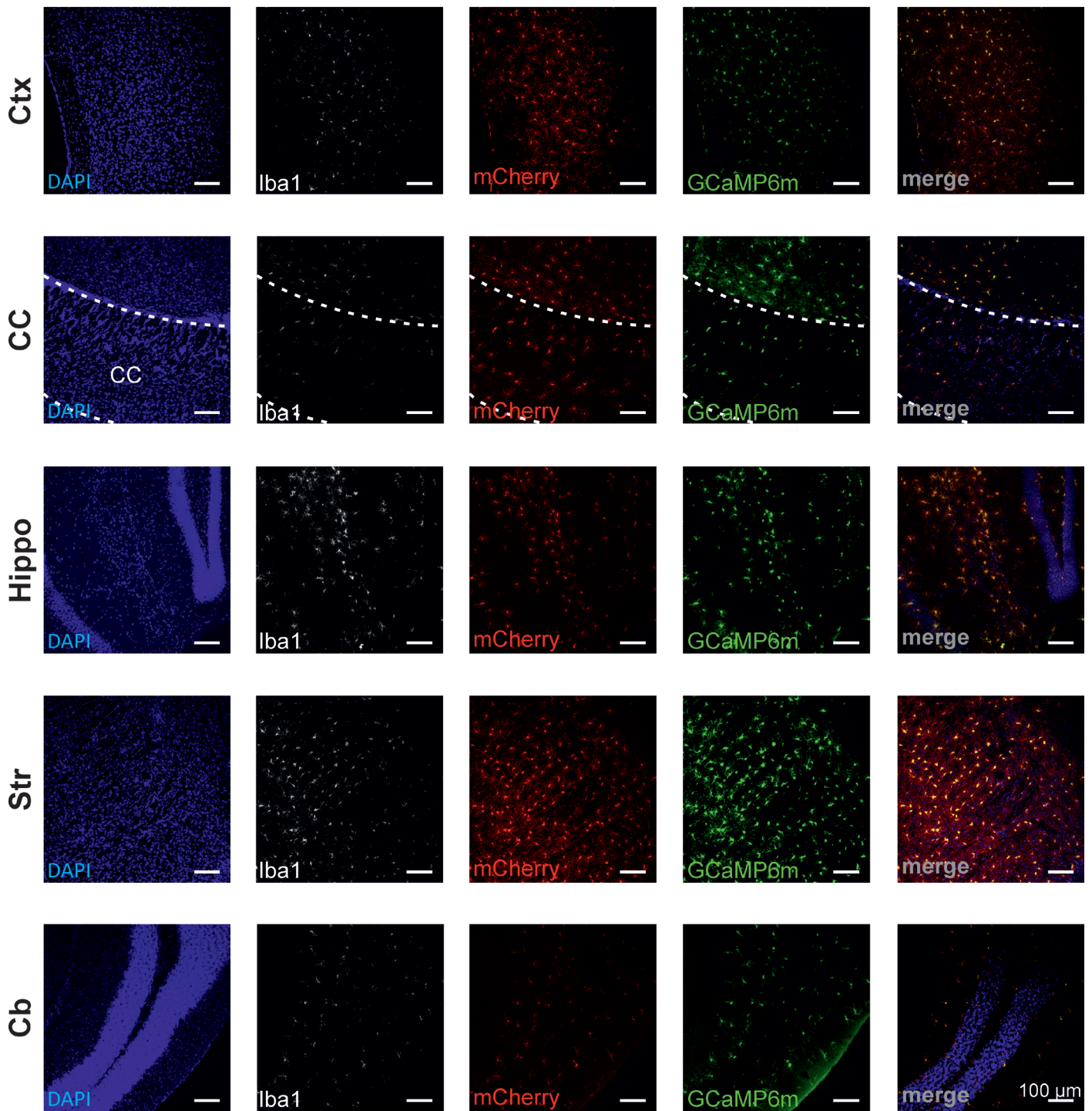
Logiacco *et al.*





**Suppl. Fig. 1 C2G mice express GCaMP6m specifically in microglia**

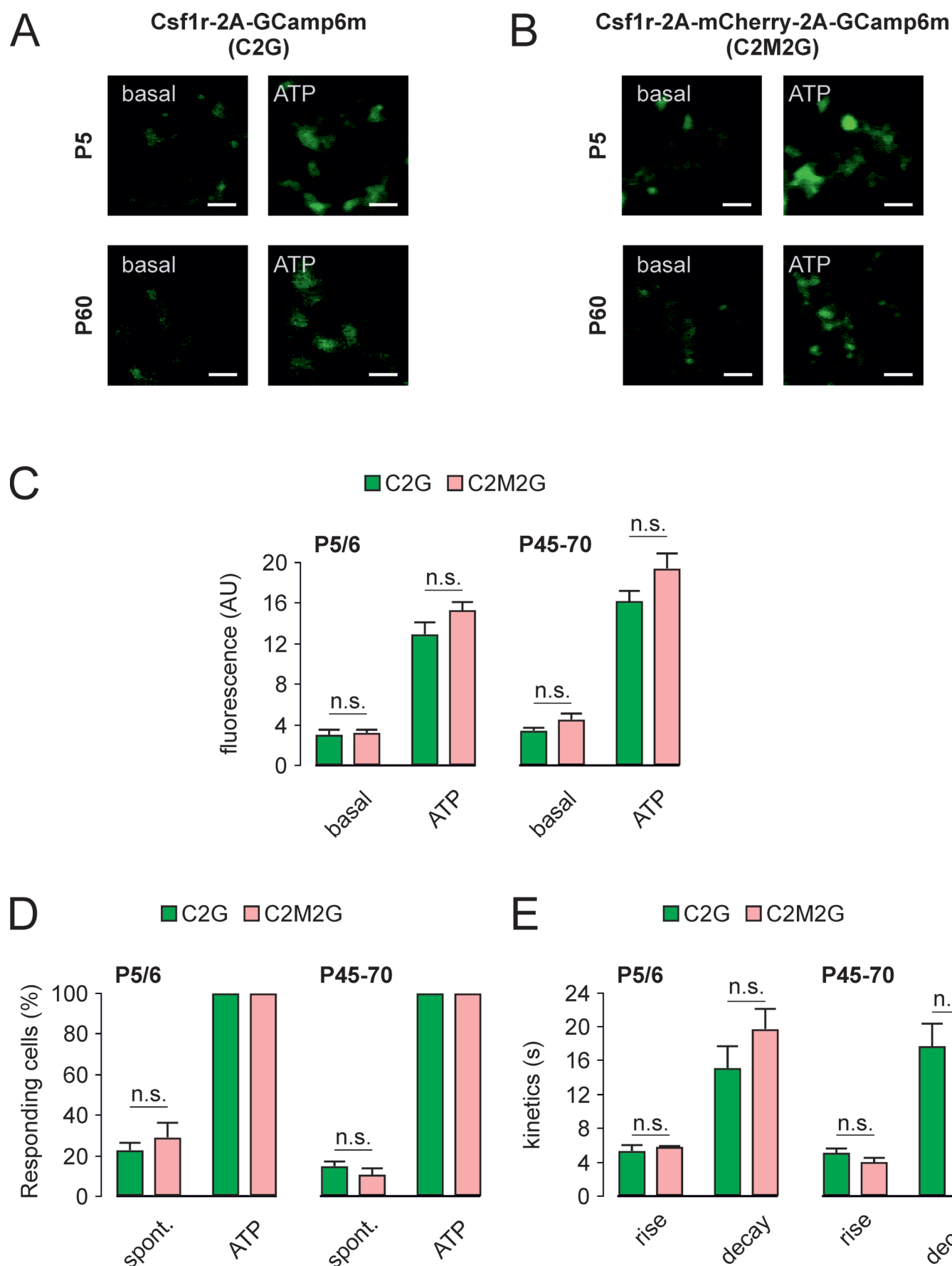
Representative confocal microscopic images (10X) of brain slices from an adult C2G mouse showing DAPI (cellular nuclei), anti-iba-1 (microglia) and anti-GFP (GCaMP6m) signals in the cortex, hippocampus, striatum, cerebellum and corpus callosum. Scale bars represent 100 μm. The images on the right show single microglial cells at higher magnification with the scale bars representing 20 μm. In all brain regions, there was a nearly 100% overlay of Iba-1 and GCaMP6m signals. n = 3 mice, 12 slices.



**Suppl. Fig. 2 C2M2G mice express GCaMP6m specifically in microglia**

Representative confocal microscopic images (10X) of brain slices from an adult C2M2G mouse showing DAPI (cellular nuclei), anti-iba-1 (microglia) anti-GFP (GCaMP6m), and anti-RFP (mCherry) signals in the cortex, hippocampus, striatum, cerebellum and corpus callosum. Scale bars represent 100  $\mu$ m. The images on the right (63X) show an extended on single microglial cells. Scale bars represent 20  $\mu$ m. In all brain regions, there was a nearly 100% overlay of Iba-1 and GCaMP6m as well as mCherry signals. n = 3 mice, 12 slices.





Suppl. Fig. 3 Comparison of microglial Ca<sup>2+</sup> level changes in C2G and C2M2G mice

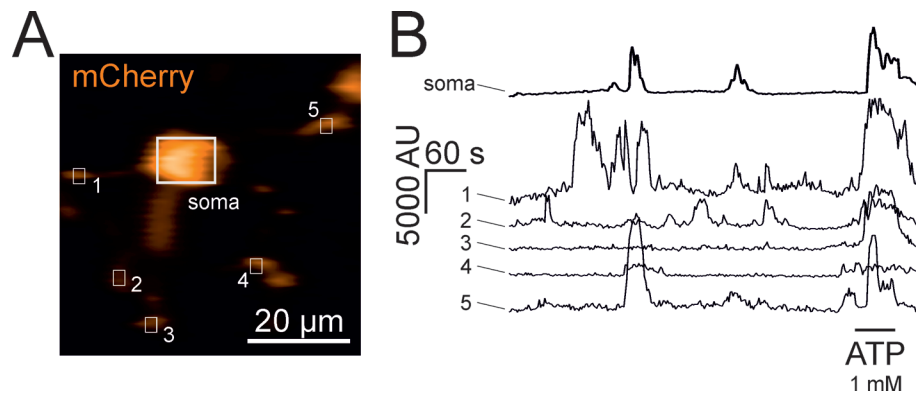
A and B. Representative images during 2-photon live cell recordings from neonatal and adult C2G (A) and C2M2G (B) hippocampal brain slices. GCaMP6m fluorescence is barely visible under control conditions ("basal") and robustly increased upon the presence of 1 mM ATP. Scale bar: 20  $\mu$ m.

C. Average GCaMP6m fluorescence in neonatal (n = 8 mice, 17 slices; 406 cells) and adult (n = 5 mice, 19 slices; 577 cells) C2G (A) and C2M2G (B) hippocampal brain slices under basal conditions and in the presence of ATP. There was no significant difference between the two mouse models.

D. Summary of the percentage of responding cells in neonatal and adult C2G and C2M2G hippocampal brain slices during 5 min under control conditions ("spont.") and upon ATP application. Responding cells were those which displayed at least one spontaneous elevation during 5 min basal recording ("spont.") or those with a  $\text{Ca}^{2+}$  elevation during ATP application. See materials and methods for thresholds. Experiments were performed and analyzed on neonatal (P5-6) and adult (P45-70) C2G and C2M2G animals. There was no significant difference between the two mouse models but an age-dependent decrease in the percentage of spontaneously active microglia. Note that ATP-responding cells are always 100% as we only considered ATP-responding cells for our analysis.

E. Summary of rise and decay times of spontaneous  $\text{Ca}^{2+}$  elevations in hippocampal microglia in neonatal and adult C2G and C2M2G mice. There was no significant difference between the two mouse models.

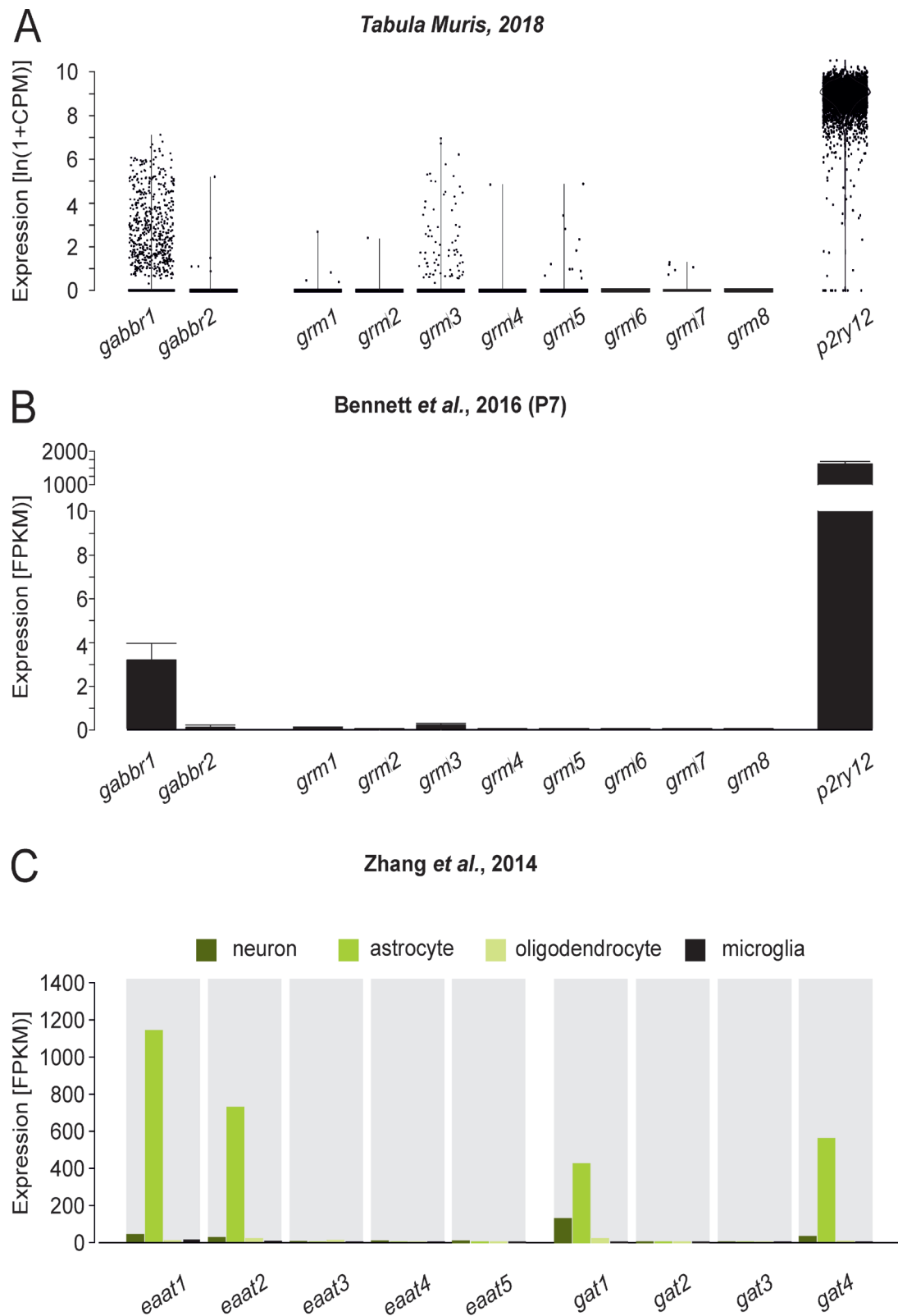
Data in C-E are presented as mean  $\pm$  SEM. Statistical significance: n.s.,  $p \geq 0.05$ ; \*,  $p \leq 0.05$ ; \*\*,  $p \leq 0.01$ , \*\*\*,  $p \leq 0.001$



**Suppl. Fig. 4 Spontaneous  $\text{Ca}^{2+}$  elevations in microglial soma and processes**

A. Confocal image of a microglial cell during a live-cell recording visualized by its fluorescence of transgenic mCherry. Regions of interest (soma and process regions 1-5) of traces in B are indicated. Scale bar: 20  $\mu\text{m}$ .

B. Basal  $\text{Ca}^{2+}$  traces and responses upon application of external ATP (1 mM). Traces were obtained from the regions of interest that are indicated in Panel A. The scaling of the amplitudes refers to a 16-bit range. Scale bar: 20  $\mu\text{m}$ .  
n = 6 mice, 9 slices.

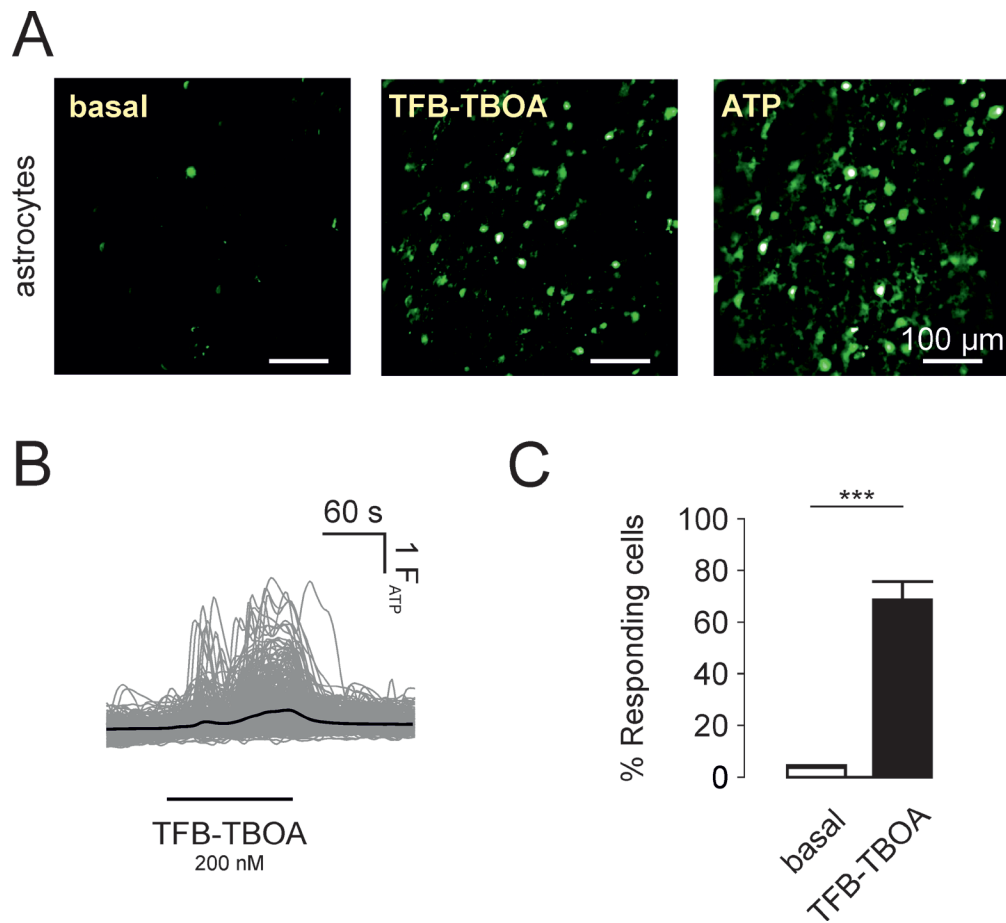


**Suppl. Fig. 5 Microglia express metabotropic GABA receptors.**

A. Meta analysis of microglial single cell mRNA expression of metabotropic GABA and glutamate receptor isoforms. Data were extracted from the Tabula Muris database (<https://tabula-muris.ds.czbiohub.org>). Note the identification of *gabbr1* in a subset of sequenced microglia.

B. Meta analysis of microglial bulk mRNA expression of metabotropic GABA and glutamate receptor isoforms at P7 (Bennett et al., 2016). As in the data in A, *gabbr1* expression was identified at low levels.

C. Meta analysis of microglial bulk mRNA expression of GABA and glutamate transporters in different brain cell types (Zhang et al., 2014).

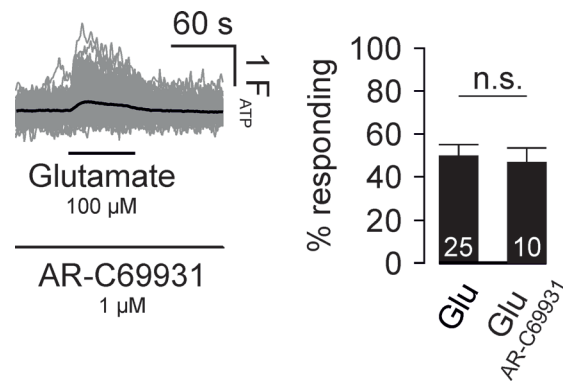


**Suppl. Fig. 6 TBOA evokes  $\text{Ca}^{2+}$  elevations in astrocytes**

A. Representative images during 2-photon live cell recordings from responding astrocytes in hippocampal brain slices. Fluo4 fluorescence images were generated by calculating a maximum projection of 60 s during substance application (or simply a 60 s basal segment) and then subtracting a background image which was taken from the projection 60s before. Scale bar: 100  $\mu$ m.

B. Astrocytic calcium traces of responding cells before, during and after TFB-TBOA (200 nm) application are shown in gray. Black traces are the average of all gray traces. TBOA application is indicated by the bar.

C. Quantification of responding astrocytes indicates a significant response of hippocampal astrocytes upon TBOA application.  $n = 4$  mice, 8 slices, 408 cells.

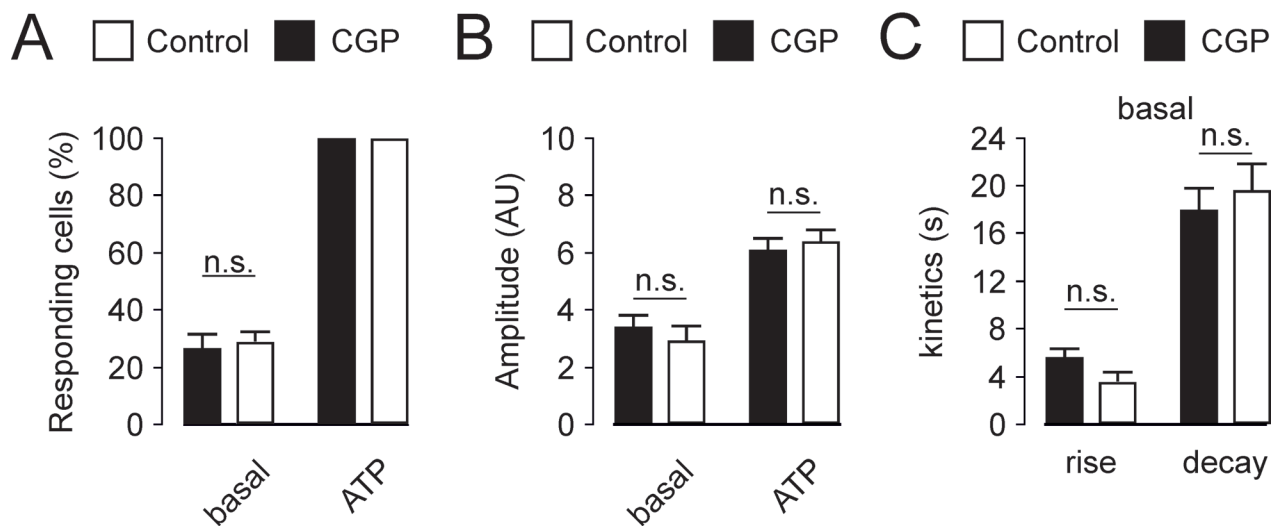


**Suppl. Fig. 7 Microglial responses upon external glutamate application are independent of P2ry12.**

On the *left*, microglial calcium traces from P5-6 hippocampal brain slices in the presence of 1  $\mu$ M AR-C69931 before, during and after glutamate application (100  $\mu$ M) are shown in gray. Black traces are the average of all gray traces. Applications are indicated by the bar.

On the *right*, quantification of glutamate-responding microglia indicates no significant effect by the blockade of P2ry12. n = 8 mice, 10 slices, 419 cells.





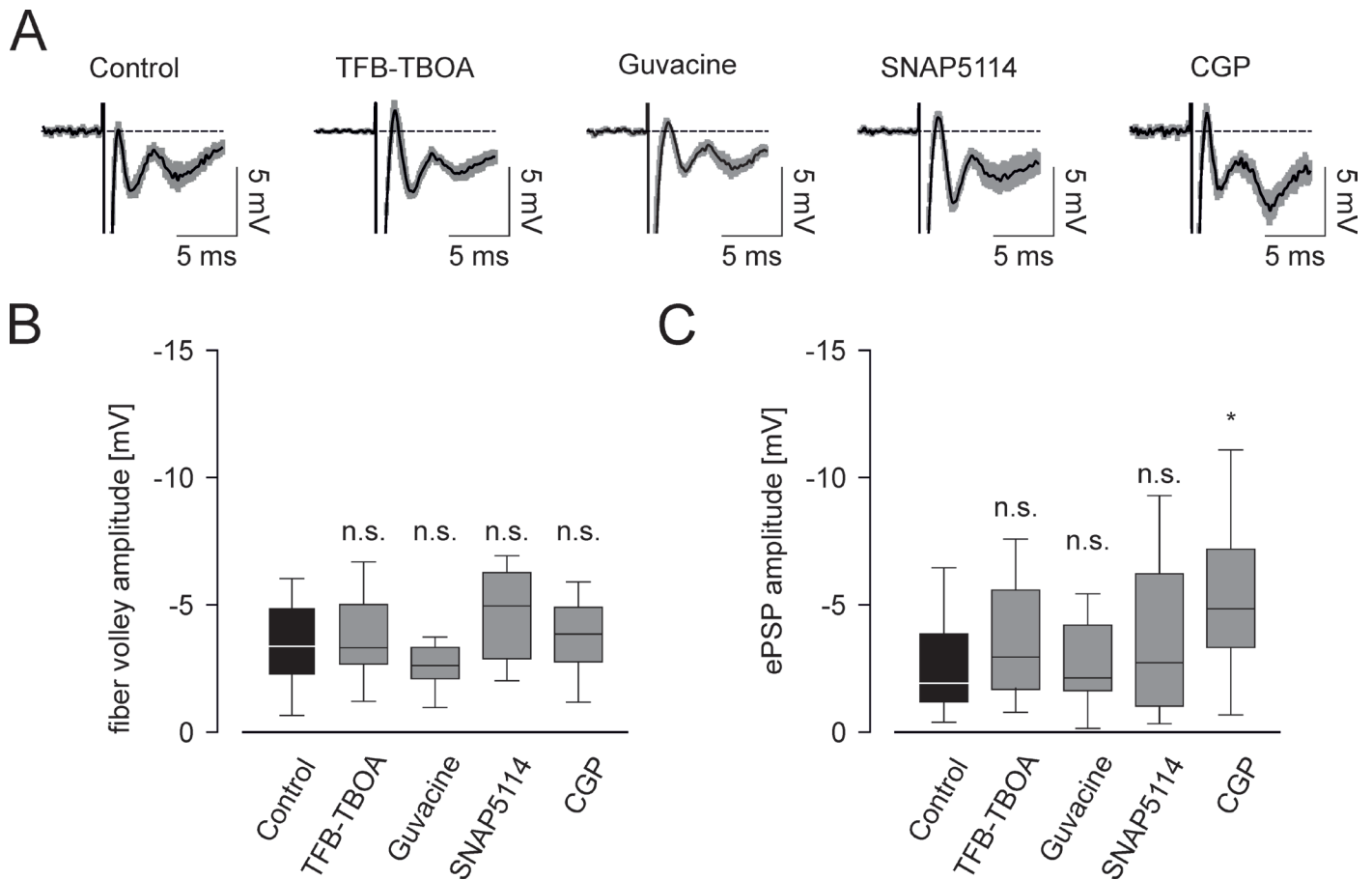
**Suppl. Fig. 8 GABA<sub>B</sub>R blockade does not affect spontaneous Ca<sup>2+</sup> elevations in microglia**

A. Summary of the percentage of basally active microglia in neonatal C2G and C2M2G hippocampal brain slices during 5 min under control conditions and in the presence of CGP55485 (1  $\mu$ M). Responding cells were those which displayed at least one spontaneous elevation during 5 min basal recording or those with a Ca<sup>2+</sup> elevation during ATP application. See materials and methods for thresholds. Experiments were performed and analyzed on neonatal (P5-6) C2G and C2M2G animals. There was no significant difference in the percentage of spontaneously active microglia between Control and CGP. Note that ATP-responding cells are always 100% as we only considered ATP-responding cells for our analysis. n = 4 mice, 10 slices, 486 cells.

B. Average amplitude of spontaneous events under control conditions, and in the presence of CGP55485 (1  $\mu$ M) as well as amplitudes evoked by 1 mM ATP.

C. Summary of rise and decay times of spontaneous Ca<sup>2+</sup> elevations in hippocampal microglia in neonatal C2G and C2M2G mice under control conditions and in the presence of CGP55485 (1  $\mu$ M). There was no significant difference between the two conditions.

Data are presented as mean  $\pm$  SEM. Statistical significance: n.s.,  $p \geq 0.05$ ; \*,  $p \leq 0.05$ ; \*\*,  $p \leq 0.01$ ; \*\*\*,  $p \leq 0.001$



**Suppl. Fig. 9 Hippocampal field potential responses in the presence of EAAT, GAT and GABA<sub>B</sub> receptor blockers.**

A. Averaged CA1 field potentials in response to the first pulse of the stimulus train under control conditions and in the presence of the EAAT1/2 inhibitor TFB-TBOA (200 nM), the GABA uptake inhibitor Guvacine (300  $\mu$ M), the GAT3-specific blocker SNAP5114 (40  $\mu$ M) and the GABA<sub>B</sub> blocker CGP55845 (1  $\mu$ M).

B. Comparison of the fiber volley amplitudes of field potential responses in the presence of the blockers (see panel A). There were no significant differences evoked by the blockade of glutamate or GABA transport or by GABA<sub>B</sub> receptor blockade.

C. Comparison of the ePSP amplitudes of field potential responses in the presence of the blockers (see panel A). There were no significant differences evoked by the blockade of glutamate or GABA transport. GABA<sub>B</sub> receptor blockade led to a significant increase in ePSPs, in accordance to previous reports (Valente et al., 2017, Sakaba and Neher, 2003, Thanawala and Regehr, 2013).